

FR-7174

**Experimental Separation and Identification of Acoustic
Normal Modes in Shallow Water**

**R.H. Ferris
F. Ingenito
A.L. Faber**

October 30, 1970

Naval Research Laboratory

DOCUMENT CONTROL DATA - R & D

(Security classification of title, body of abstract and indexing annotation must be entered when the overall report is classified)

1. ORIGINATING ACTIVITY (Corporate author) Naval Research Laboratory Washington, D.C. 20390		2a. REPORT SECURITY CLASSIFICATION Unclassified	
		2b. GROUP NA	
3. REPORT TITLE EXPERIMENTAL SEPARATION AND IDENTIFICATION OF ACOUSTIC NORMAL MODES IN SHALLOW WATER			
4. DESCRIPTIVE NOTES (Type of report and inclusive dates) Interim report; work is continuing on the problem.			
5. AUTHOR(S) (First name, middle initial, last name) Raymond H. Ferris, Frank Ingenito, and Andrew L. Faber			
6. REPORT DATE October 30, 1970		7a. TOTAL NO. OF PAGES 34	7b. NO. OF REFS 4
8a. CONTRACT OR GRANT NO. NRL Problem S01-45		9a. ORIGINATOR'S REPORT NUMBER(S) NRL Report 7174	
b. PROJECT NO. RF 05-552-404-5350			
c. SF 11-552-001-14275		9b. OTHER REPORT NO(S) (Any other numbers that may be assigned this report)	
d.			
10. DISTRIBUTION STATEMENT This document has been approved for public release and sale; its distribution is unlimited.			
11. SUPPLEMENTARY NOTES		12. SPONSORING MILITARY ACTIVITY Department of the Navy (Office of Naval Research, Arlington, Va. 22217), and Naval Ship Systems Command, Wash. D.C.	
13. ABSTRACT Normal-mode models of ducted propagation require knowledge of the attenuation coefficients for each mode in order to predict signal intensities. An experiment was conducted in the Gulf of Mexico in July 1969 to evaluate a technique for isolating, identifying, and measuring the intensity of signals propagated in individual normal modes. The measurements were made under downward refracting conditions in 30 meters of water with a level sand bottom. By projecting short (3-cycle) pulses and listening at a sufficiently long range, the differing group velocities of the modes permitted resolution of some individual mode arrivals. The resolved modes were identified by comparing the measured vertical intensity distributions and relative group velocities with those predicted by a normal-mode model. The model used assumes a semi-infinite, lossless, fluid bottom of constant velocity overlain with a constant-depth water layer having an arbitrary velocity profile. At 400 Hertz the observed intensity distributions and relative group velocities for the first two modes were in excellent agreement with predicted values. Results at higher frequencies were inconclusive, since the prevailing sound-speed profiles did not permit resolution of any individual modes. Results of this experiment show that the short-pulse technique is a practical means of making direct measurements of modal attenuation. Although not every mode is resolvable under each set of environmental conditions, measurements made on those which are resolvable should serve to validate other less direct methods of measurement.			

14. KEY WORDS	LINK A		LINK B		LINK C	
	ROLE	WT	ROLE	WT	ROLE	WT
Underwater acoustics Shallow water Normal modes Attenuation Prediction Acoustic propagation						

CONTENTS

Abstract	ii
Problem Status	ii
Authorization	ii
INTRODUCTION	1
THEORY	3
EXPERIMENTAL PROCEDURE	6
Acoustic Sources	6
Hydrophone Deployment	6
Recording Instrumentation	6
Signal Programming	8
Oceanographic Measurements	8
Range Limitation	8
RESULTS	8
CONCLUSIONS	16
ACKNOWLEDGMENTS	17
REFERENCES	17
APPENDIX A - The Normal-Mode Program	18
APPENDIX B - Oceanographic Measurements	20

ABSTRACT

Normal-mode models of ducted propagation require knowledge of the attenuation coefficients for each mode in order to predict signal intensities. An experiment was conducted in the Gulf of Mexico in July 1969 to evaluate a technique for isolating, identifying, and measuring the intensity of signals propagated in individual normal modes. The measurements were made under downward refracting conditions in 30 meters of water with a level sand bottom. By projecting short (3-cycle) pulses and listening at a sufficiently long range, the differing group velocities of the modes permitted resolution of some individual mode arrivals. The resolved modes were identified by comparing the measured vertical intensity distributions and relative group velocities with those predicted by a normal-mode model. The model used assumes a semi-infinite, lossless, fluid bottom of constant velocity overlain with a constant-depth water layer having an arbitrary velocity profile. At 400 Hz the observed intensity distributions and relative group velocities for the first two modes were in excellent agreement with predicted values. Results at higher frequencies were inconclusive, since the prevailing sound-speed profiles did not permit resolution of any individual modes. Results of this experiment show that the short-pulse technique is a practical means of making direct measurements of modal attenuation. Although not every mode is resolvable under each set of environmental conditions, measurements made on those which are resolvable should serve to validate other less direct methods of measurement.

PROBLEM STATUS

This is an interim report; work on the problem is continuing.

AUTHORIZATION

NRL Problem S01-45
Projects RF 05-552-404-5350 and SF 11-552-001-14275

Manuscript submitted August 4, 1970.

EXPERIMENTAL SEPARATION AND IDENTIFICATION OF ACOUSTIC NORMAL MODES IN SHALLOW WATER

INTRODUCTION

In a simple normal-mode model of acoustic propagation in shallow water, the signal field consists of the sum of signals propagated in each of the normal modes of the duct. Since the signal attenuation can be expected to vary from mode to mode, a useful prediction model must consider modal attenuation.

Attenuation coefficients for individual modes can be determined, at least in theory, indirectly from measurements of the total signal field (1a)*. There are, however, at least two possible techniques for isolating individual modes to allow direct measurement of modal attenuation. It is possible in principle to design a source or receiving array which excites or responds to signals in only one mode. An obvious experimental difficulty with this method is that the array would have to be restructured for changes in mode number, water depth, sound-speed profile, or bottom type. A second method is suggested by the property of ducted propagation that the group velocity associated with each mode is a function of frequency and that the velocities are not the same for all modes. By projecting short pulses and listening with an array of hydrophones at a sufficiently large range, one can as a consequence of the differing group velocities of the modes resolve some individual mode arrivals. The resolved modes can be identified by comparing the measured vertical intensity distributions and relative group velocities with those predicted by a model.

To resolve a signal which has been propagated via a single normal mode the propagation time for that mode must differ from the propagation time of temporally adjacent modes by a time equal to the length of the transmitted pulse plus any time smearing of the pulse due to dispersion. A predictive model which provides a reasonably accurate estimate of the group velocities as a function of frequency and the vertical distribution of intensity for each of the possible normal modes is indispensable for designing the experiment and for selecting and identifying modes. The group-velocity functions are particularly sensitive to changes in the sound-speed profile. Small variations in profile can result in changes in the relative arrival times and even in the order of arrival of modes. Dispersive spreading, caused by variation of the group velocity within the bandwidth of the signal, affects the duration and amplitude of received signals and hence affects the resolvability of modes and the signal-to-noise ratio.

An experiment was conducted during the period July 21 through August 2, 1969, in the Gulf of Mexico to evaluate the second, or dispersion, method of mode resolution and to obtain experimental values of mode attenuation coefficients. Since this method requires a model to predict mode intensity profiles and group velocities, the evaluation also serves as a test of the adequacy of the model. Three variable-depth acoustic sources were deployed from a fixed tower, a Naval Ship Research and Development Laboratory, Panama City, facility known as Stage I. This tower stands in 30 meters of water approximately 20 kilometers offshore from Panama City, Florida, at $30^{\circ}00'06''$ N and $85^{\circ}54'02''$ W (Fig. 1). Source center frequencies were 400, 750, and 1500 Hz, and each source was essentially omnidirectional.

*A complete account of normal-mode theory can be found in this reference.

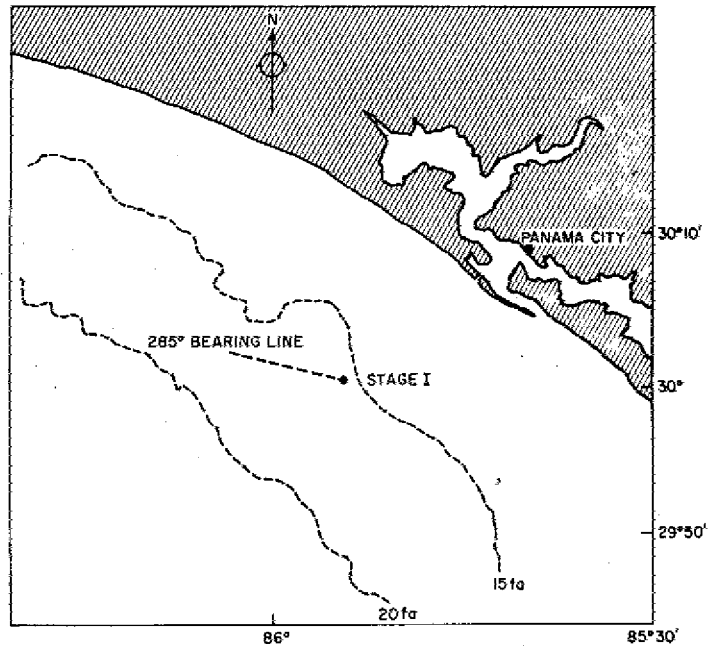


Fig. 1 - Operations area near Panama City, Florida

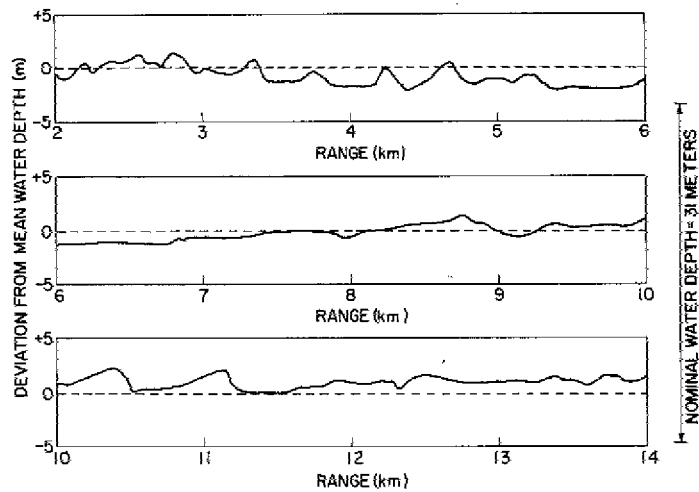


Fig. 2 - Bottom profile along the 285-degree bearing line from Stage I

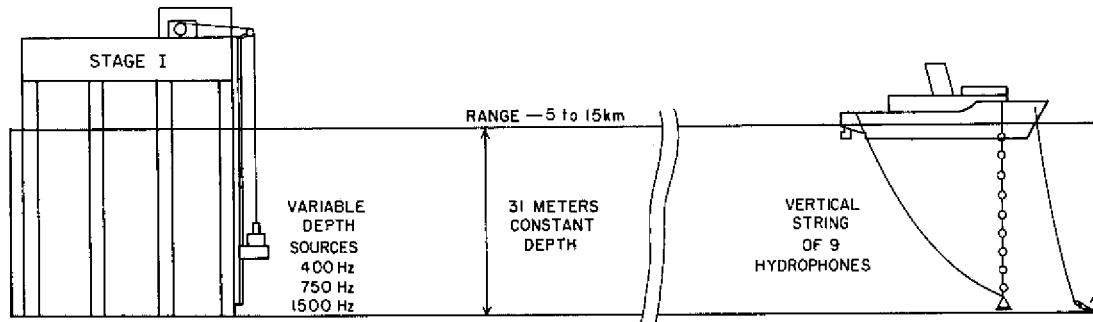


Fig. 3 - Experimental setup. The constant depth shown actually varied along the bearing line as shown in Fig. 2, and the depth value of 31 meters had a tidal variation of about 1 meter.

In an effort to find a bearing line having a minimum of depth variation, several bathymetric runs were made to 16 kilometers on constant bearing lines from Stage I. The 285-degree bearing line, having a nominal depth of 31 meters and the bottom profile illustrated in Fig. 2, was selected, and all acoustic data were taken on this bearing. The actual water depth depends on tidal conditions; the maximum tidal variation observed at Stage I during the experiment was approximately 1 meter.

A vertical string of nine hydrophones was suspended from the anchored receiving ship, the USNS *Gibbs* (T-AGOR-1). The hydrophones were spaced at 3-meter intervals, with the uppermost hydrophone submerged to a depth of 3 meters. Figure 3 illustrates the experimental geometry. The source levels and propagation loss were such that an adequate signal-to-noise ratio could not be obtained for ranges greater than 15 kilometers.

THEORY

An acoustic pulse propagating in shallow water is subject to losses due to cylindrical spreading and dispersion, and the excitation of the individual modes depends on the positions of the source and receiver. If these effects are accounted for, the mode attenuation coefficients can be computed from measurements of the pressure amplitudes of individual modes.

The conditions of the present experiment are approximated by a water layer of constant total depth H , constant density ρ_1 , and a sound velocity $c_1(z)$ which is a function of depth z . The water layer is bounded above by air and below by a semi-infinite fluid of constant density ρ_2 and constant sound velocity c_2 . A point source of unit source strength and angular frequency ω is located at a depth z_0 in the water (Fig. 4). Later, corrections will be made for a pulsed source and for attenuation. The receiver is located at a depth z , with r being the horizontal distance between source and receiver.

At long ranges the velocity potential $\phi(r, z)$, after dropping the time dependence $e^{-i\omega t}$, is found (1b) to be

$$\phi(r, \zeta) = i \left(\frac{1}{8\pi r} \right)^{1/2} \frac{\rho_1}{H} \sum_{n=1}^M \frac{u_n(\zeta_0) u_n(\zeta)}{k_n^{1/2}} e^{i[k_n r - (\pi/4)]}, \quad (1)$$

where $\zeta = z/H$ is the normalized depth, k_n is the horizontal component of the wave number of the n th mode, and M is the number of discrete modes. The $u_n(\zeta)$ are defined as

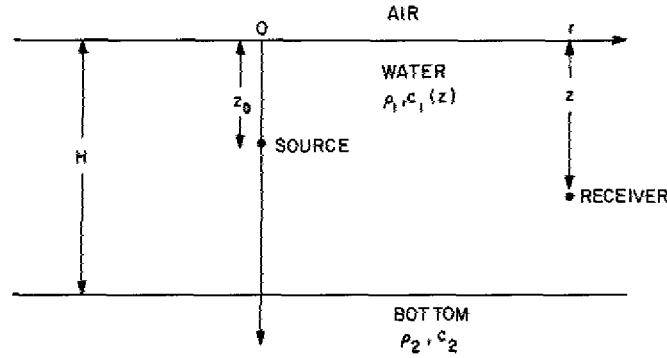


Fig. 4 - Cylindrical coordinate system used in the model. The water layer of constant depth H and density ρ_1 , and variable sound speed $c_1(z)$ is bounded above by air and below by the bottom of constant density ρ_2 and sound speed c_2 .

$$u_n(\zeta) = N_n Z_n^{(1)}(\zeta), \quad 1 \geq \zeta \geq 0, \quad (2a)$$

$$= N_n Z_n^{(2)}(\zeta), \quad \infty > \zeta \geq 1, \quad (2b)$$

where the N_n are the normalization constants obtained from the conditions

$$N_n^2 \left\{ \int_0^1 \rho_1 [Z_n^{(1)}(\zeta)]^2 d\zeta + \int_1^\infty \rho_2 [Z_n^{(2)}(\zeta)]^2 d\zeta \right\} = 1, \quad (3)$$

and the $Z_n^{(1),(2)}(\zeta)$ and the k_n are solutions of the equations

$$\frac{d^2 Z_n^{(1)}}{d\zeta^2} + H^2 \left(\frac{\omega^2}{c_1^2(\zeta)} - k_n^2 \right) Z_n^{(1)} = 0, \quad 1 \geq \zeta \geq 0, \quad (4a)$$

$$\frac{d^2 Z_n^{(2)}}{d\zeta^2} + H^2 \left(\omega^2/c_2^2 - k_n^2 \right) Z_n^{(2)} = 0, \quad \infty > \zeta \geq 1, \quad (4b)$$

with the boundary conditions

$$Z_n^{(1)}(0) = 0, \quad (5a)$$

$$\rho_1 Z_n^{(1)}(1) = \rho_2 Z_n^{(2)}(1), \quad (5b)$$

and

$$\left. \frac{dZ_n^{(1)}}{d\zeta} \right|_{\zeta=1} = \left. \frac{dZ_n^{(2)}}{d\zeta} \right|_{\zeta=1} \quad (5c)$$

Equation (5a) requires that the acoustic pressure vanish at the air/water interface, and Eqs. (5b) and (5c) require that the acoustic pressure and the normal component of the particle velocity be continuous at the bottom boundary.

Equation (1) represents the signal field at long ranges as the sum of a finite number of discrete terms, each term corresponding to one of the normal modes of the system. The first mode has no zeros except at the surface, and each higher mode has one more

zero than its immediate predecessor. A computer program has been written which solves Eqs. (3), (4), and (5) numerically and obtains the mode amplitudes $u_n(\zeta)$ and wave numbers k_n for a generalized velocity profile $c_1(\zeta)$. For use with pulsed sources the program also calculates the group velocities U_n , given by

$$U_n = \frac{\partial \omega}{\partial k_n}. \quad (6)$$

Details are given in Appendix A.

The pressure amplitude of each mode at range r is given by

$$P_n(r, \zeta) = \frac{\omega \rho_1^2}{H} \left(\frac{1}{8\pi r} \right)^{1/2} \frac{U_n(\zeta_0) U_n(\zeta)}{k_n^{1/2}}, \quad 0 \leq \zeta \leq 1. \quad (7)$$

Two corrections must be made to Eq. (7). The right side must be multiplied by the factor $e^{-\delta_n r}$, where δ_n is the mode attenuation coefficient (1c). This factor expresses the effect of the losses in the system on an individual mode. In addition, for a pulsed source account must be taken of the lengthening of the propagating pulse and consequent decrease in pressure amplitude with range due to dispersion in the system. We can make an approximate correction for this by noting that there is no additional energy loss due to dispersion. Then we assume, as for a square pulse, that the square of the pressure amplitude of a normal-mode component of the propagating pulse is inversely proportional to the pulse length. Thus, the right-hand side of Eq. (7) must be multiplied by $[T_0/(T_0 + \Delta T_n)]^{1/2}$, where T_0 is the pulse length at the source and ΔT_n is the change in pulse length at range r . Making these corrections in Eq. (7) gives

$$P_n(r, \zeta) = \frac{\omega \rho_1^2}{H} \left(\frac{1}{8\pi r} \right)^{1/2} \frac{U_n(\zeta_0) U_n(\zeta)}{k_n^{1/2}} \left(\frac{T_0}{T_0 + \Delta T_n} \right)^{1/2} e^{-\delta_n r}. \quad (8)$$

In the MKS system of units ρ_n is in newtons/meter².

To introduce the source level S in decibels relative to 1 dyne/cm² at 1 meter we note that close to the source the pressure should be

$$p(r, z) = \frac{-i \omega \rho_1}{4\pi} \frac{e^{ik\sqrt{r^2+z^2}}}{\sqrt{r^2+z^2}}, \quad (9)$$

which, at 1 meter, gives a pressure amplitude of $\omega \rho_1/4\pi$ in newtons/meter². Thus, Eq. (8) is the pressure due to a source level of $20 \log(10\omega \rho_1/4\pi)$ relative to 1 dyne/cm² at 1 meter, where the factor of 10 enters because of the conversion from newtons/meter² to dynes/centimeter². Converting Eq. (8) to decibels relative to 1 dyne/cm² and adding the term $S - 20 \log(10\omega \rho_1/4\pi)$ we get

$$\begin{aligned} 20 \log P_n = & S + 20 \log \left[\frac{\sqrt{2\pi}}{H} \frac{\rho_1 U_n(\zeta_0) U_n(\zeta)}{k_n^{1/2}} \right] - 10 \log r \\ & + 10 \log \left(\frac{T_0}{T_0 + \Delta T_n} \right) - \alpha_n r, \end{aligned} \quad (10)$$

where the new source level is S and

$$\alpha_n = (20 \log e) \delta_n. \quad (11)$$

In using Eq. (10) each of the products $\alpha_n r$, $k_n r$, and $\rho_1 u_n(\zeta) u_n(\zeta_0)$ may be taken in any consistent set of units, but S must be in decibels relative to 1 dyne/cm² at 1 meter and H must be in meters. Then $20 \log p_n$ will be in decibels relative to 1 dyne/cm².

In the present experiment all the terms of Eq. (10) are measured or calculated with the exception of α_n , which can then be determined.

EXPERIMENTAL PROCEDURE

Acoustic Sources

Three acoustic sources were lowered on rails down the southwest side of Stage I. The source depth could be continuously varied from zero to a maximum depth dictated by the length of the rails, the relative positions in which the three sources were mounted, and the tide level. The nominal maximum depths were 22.5, 24.5, and 23 meters for the 400-, 750-, and 1500-Hz sources respectively. All sources were essentially omnidirectional. Signal waveforms consisted of sine waves gated on for 3, 4, or 63 cycles. The mechanical Q's of the sources were such that the acoustic signals could not build up to full output with the 3- or the 4-cycle pulses. Source levels, as determined with a calibrated hydrophone at Stage I, were as shown in Table 1. In the case of the 3- and 4-cycle pulses the tabulated source levels correspond to the maximum buildup of the source output.

Table 1
Source Levels

Pulse Length (cycles)	Source Level (dB rel. 1 dyne/cm ² at 1 meter)		
	400 Hz	750 Hz	1500 Hz
3	95.4	99.4	93.4
4	96.9	99.4	96.9
63	99.3	105.3	102.1

In all cases the signal gated into the driver amplifier started and ended on a positive-going axis crossing. The 3- and 4-cycle pulses were used when examining individual normal modes, and the 63-cycle pulses were used to examine the sum of the modes.

Hydrophone Deployment

A vertical string of nine hydrophones was suspended from a davit on the starboard bow of the receiving ship. The hydrophones were separated at uniform intervals of 3 meters, with the uppermost unit submerged to a depth of 3 meters. A 600-pound lead weight fastened to the end of the supporting wire rope, 1 meter below the lowest hydrophone, kept the string in a vertical position. No evidence of streaming was observed. The lead weight was lifted to the stern of the ship for transiting.

Recording Instrumentation

A block diagram of the recording equipment used on the *Gibbs* is shown in Fig. 5. Signals from the nine hydrophones passed through coaxial cables 90 meters long to the laboratory, where they were amplified, filtered in 1/2-octave bands centered on 400, 750,

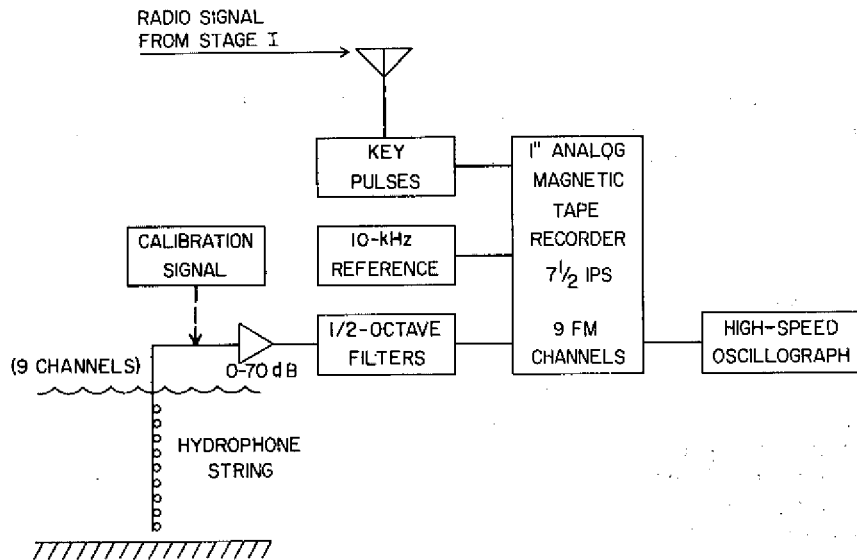


Fig. 5 - Shipboard recording instrumentation

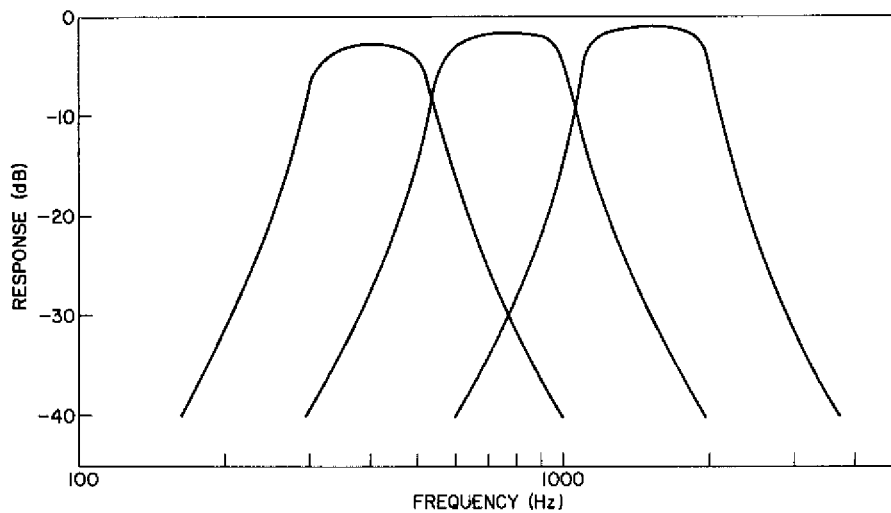


Fig. 6 - Voltage response of the 1/2-octave filters centered on 400, 750, and 1500 Hz

or 1500 Hz (filter response curves are shown in Fig. 6), and recorded on nine FM channels of a 1-inch magnetic tape recorder operated at 7.5 ips. Key pulses sent by radio from Stage I simultaneously with the acoustic pulses were also recorded, as was a 10-kHz reference frequency. A multichannel, high-speed oscillographic recorder was used for shipboard monitoring of the signals. For each acoustic run a calibration signal was connected to the inputs of the amplifiers in place of the hydrophones and recorded on magnetic tape.

Signal Programming

When the receiving ship was anchored at any given range station and ready to record data, the source would be programmed to transmit 400-Hz, 63-cycle pulses for 7 minutes followed by 3- or 4-cycle pulses for 7 minutes. This sequence would then be repeated at 750 and 1500 Hz. Identifying run numbers were assigned to sequential blocks of data recorded on the magnetic tapes.

Oceanographic Measurements

Oceanographic instrumentation on the receiving ship consisted of a precision depth recorder (PDR), two shallow-water bathythermographs (BT's), one velocimeter, one set of Nansen bottles with reversing thermometers, and one salinometer. One shallow-water BT and a resistance-type wave staff were located on Stage I. Frequent sound-speed and temperature profiles, from the surface to the bottom, were obtained on the receiving ship during the course of the experiments. The reversing thermometers on the Nansen bottles provided a calibration check for the BT's. The velocimeter was the most frequently used instrument for obtaining sound-speed profiles. It was repeatedly calibrated from sound speed calculated from salinity, temperature, and pressure obtained from Nansen casts and BT's taken simultaneously with a velocimeter cast. All temperature, salinity, and sound-speed data are presented in Appendix B. The analog voltage output of a resistance-type wave staff on Stage I was recorded on a frequency modulation channel of a tape recorder at selected intervals during the experiments. These data are also contained in Appendix B.

Range Limitation

The source levels available for this experiment provided marginal signal-to-noise ratios. For signals which are not strongly dispersed the ability to resolve modes increases with range. With the limitation on range imposed by the signal-to-noise ratio, only fortuitously configured modes could be isolated. It was not until the final days of the exercise that the first and second modes at 400 Hz were positively identified. However, once identified, they were observed in previously recorded data.

RESULTS

An individual normal mode of propagation can be identified in principle by the number of zeros in its pressure amplitude as the receiver depth is varied. Because a finite number of receivers spaced throughout the water column was used in the experiment, identification is made easier if the approximate shape of the mode and its arrival time are known. For the present experiment this information was provided by the NRL normal-mode program, described in Appendix A. For each run the appropriate frequency, velocity profile, and water depth, corrected for tidal variation, were used to obtain a set of mode-amplitude and group-velocity curves which were applied to the analysis of the run.

Figure 7 is a sample received pressure signal at 400 Hz taken from run 12-2, showing oscillograph traces of the outputs of the nine hydrophones. The first arrival has maxima at 9 and 27 meters and a single zero at about 21 meters. Close inspection of the figure indicates that the pressure amplitude undergoes a 180-degree change of phase after passing through the zero. The pressure amplitude of the second arrival increases with depth, reaching a maximum at 27 meters, with no phase changes. The sound speed profile measured during run 12-2 (BT 67, N 14) is shown in Fig. 8, and Figs. 9 and 10 show the calculated mode amplitudes $u_n(z)$ for 400 Hz and modal group velocities as a function of frequency. The calculations were performed using the values $c_2 = 1589$ m/sec and $\rho_2 =$

1.85 g/cm³ previously obtained by a bottom reflection method (2). It follows from Eq. (7) that the pressure amplitude of the n th mode should have the same variation with z as does $u_n(z)$. Comparison of Fig. 7 with Fig. 9 indicates qualitative agreement between observed and calculated pressure variation. The group velocities of Fig. 10 predict that at 400 Hz the second mode will arrive first, followed by the first mode, and that the second mode will be more dispersed than the first. Figure 11 shows the same signal as Fig. 7 with lines added to indicate the calculated times of arrival of the second mode relative to the first, and the pulse length for each mode. The transmitted pulse length was assumed to be equal to the reciprocal of the source bandwidth to the 3-dB points. The pulse lengths delineated in Fig. 11 are equal to the length of the transmitted pulse plus increments, to account for dispersion, equal to the calculated differences in arrival time for frequency components at the edges of the band. These predictions are in reasonable agreement with the measurements, confirming the identification of the first two modes. The third mode was not observed, possibly because the attenuation of the third mode is greater than that of the first two modes and because the very high third-mode dispersion indicated by the large slope of the group velocity curve at 400 Hz degrades the peak pressure still further. The fourth mode is very close to cutoff at 400 Hz, so its attenuation and dispersion are even greater than those of the third mode.

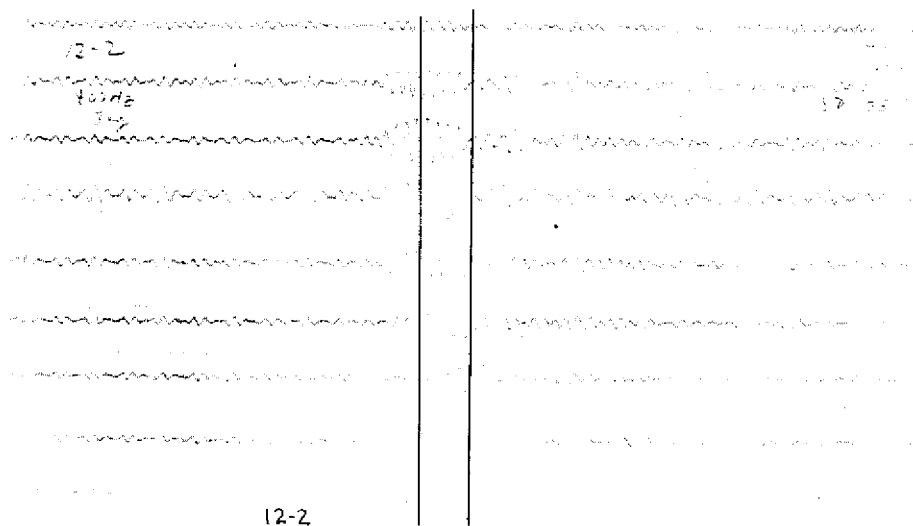


Fig. 7 - High-speed oscillographic recording of a 400-Hz 3-cycle pulse received during run 12-2. The range from the source was 11 km, and the source depth was 22.3 m. Time increases to the right; the timing marks at the top are 20 msec apart. The upper signal trace is from the hydrophone at a depth of 3 meters, the next trace down is from the hydrophone at 6 meters, and so on down to 27 meters. The vertical lines allow the phase of each arrival as a function of depth to be observed.

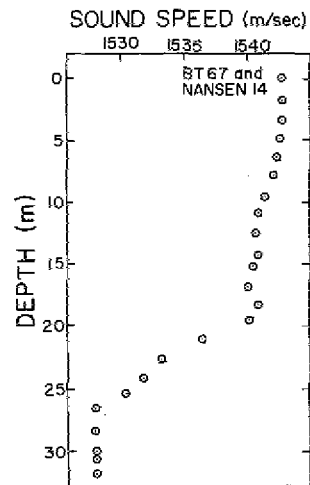
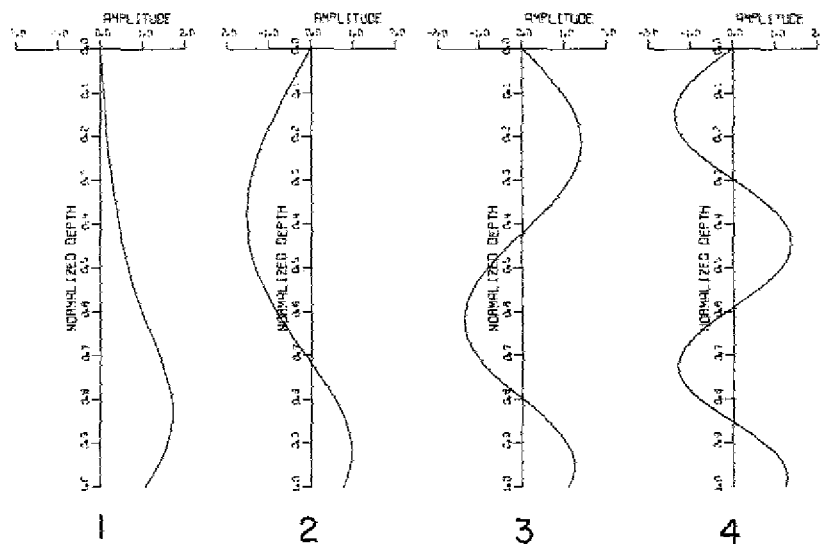


Fig. 8 - Sound speed profile measured during run 12-2



400 Hz

Fig. 9 - Mode amplitudes $u_n(z)$ at 400 Hz for the sound-speed profile of run 12-2 calculated by the normal-mode program. The vertical scale is normalized depth in the water column.

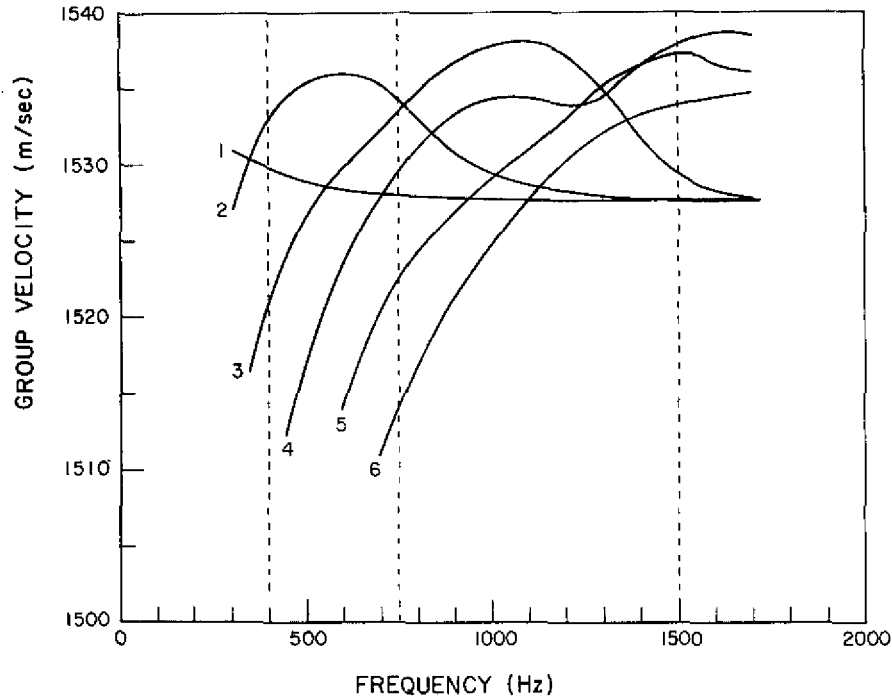


Fig. 10 - Group velocities for the first six modes for the sound speed profile of run 12-2 calculated by the normal-mode program

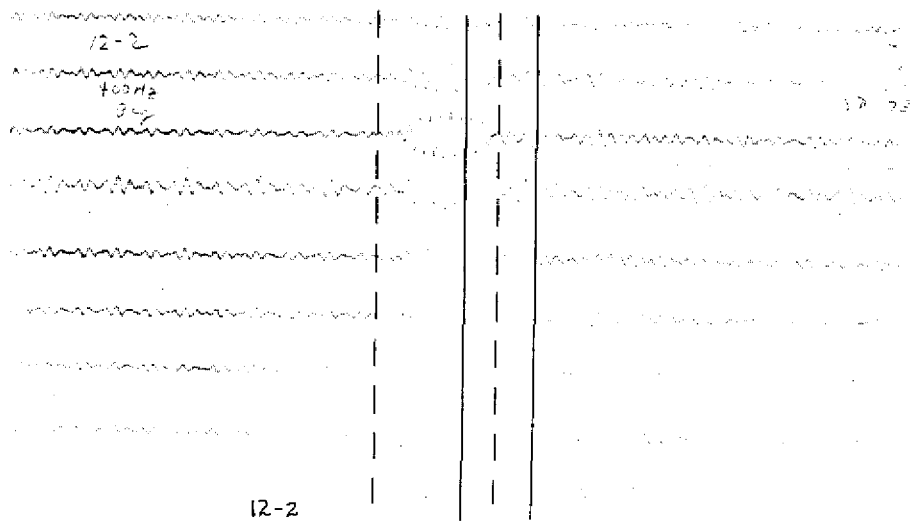


Fig. 11 - Calculated arrival times and pulse widths for the same pulse as Fig. 7. The solid lines indicate the calculated width of the first mode, and are centered on the second arrival. The dashed lines indicate the calculated width of the second mode. Their position was determined from the calculated arrival time of the second mode relative to the first.

Table 2
Summary of 400-Hz Measurements and Calculations

Experimental Parameters						Analytical Adjustments			Measured Signal Level			Corrected Signal (dB rel. 1 dyne/cm ²)
Range (km)	Source Depth (m)	Run No.	Date and Time (CDT)	Sound- Speed Profile	Mode	Mode Excitation Function (dB rel. 1 dyne/cm ²)	Dispersive Spreading (dB)	Cylindrical Spreading (dB)	No. of Samples	\bar{X}_i (dB rel. 1 dyne/cm ²)	$\frac{\bar{X}_i + \sigma}{\bar{X}_i}$ (dB)	
5.0	22.5	1-6	7/27 1432	Vel. 15	1	-17.9	-2.1	-37.0	17	26.6	1.7	83.6
					2	-35.0	-5.5	-37.0	16	22.2	2.0	99.7
5.0	20.8	2-1	7/27 1530	Vel. 15	1	-19.5	-0.8	-37.0	13	29.6	1.8	86.9
					2	-25.5	-2.2	-37.0	13	26.6	2.7	91.3
5.7	22.2	6-5	7/30 0800	Vel. 20	1	-18.0	-1.2	-37.6	15	27.1	1.0	83.9
					2	-33.5	-3.1	-37.6	15	21.1	1.8	95.3
7.3	22.3	6-1	7/29 1900	Vel. 19	1	-16.9	-0.8	-38.6	14	32.6	0.8	88.9
					2	-37.5	-1.8	-38.6	14	23.2	1.2	101.1
7.3	22.6	9-6	8/1 1143	BT 61 N 13	1	-17.1	-1.9	-38.6	13	25.3	1.3	82.9
					2	-41.3	-6.4	-38.6	13	20.6	1.4	106.9
7.5	22.6	11-5	8/2 1250	Vel. 26	1	-17.5	-2.1	-38.8	15	26.8	0.6	85.2
					2	-39.4	-11.1	-38.8	15	19.6	1.1	108.9
11.0	22.3	12-2	8/2 1820	BT 67 N 14	1	-18.4	-5.1	-40.4	29	14.2	2.0	78.1
					2	-39.6	-10.7	-40.4	29	14.9	2.4	105.6
14.6	22.5	11-3	8/1 1955	Vel. 25	1	-17.9	-5.1	-41.7	37	9.1	1.7	73.8
					2	-35.9	-10.1	-41.7	-	-	-	-

In a similar way the two lowest modes were identified and the pressure amplitudes measured for the other 400-Hz runs listed in Table 2. For all the runs the pressure amplitudes of the first and second modes were measured on the 21-meter hydrophone and the 9-meter hydrophone, respectively. To obtain \bar{X}_i , the mean value of the pressure amplitude of the i th mode for a particular run, the pressure amplitudes of the number of samples indicated in Table 2 were measured and averaged. These are shown, together with $(\bar{X}_i + \sigma)/\bar{X}_i$, where σ is the standard deviation about the mean, under the heading "Measured Signal Level," both being expressed in decibels. The value \bar{X}_i is the measured average of the p_n of Eq. (10). Since the runs were made under different conditions, they were brought into correspondence by making the corrections shown under the heading "Analytical Adjustments." The table headings are related to the terms of Eq. (10) as follows:

$$\text{mode excitation function} = 20 \log \left[\rho_1 \frac{\sqrt{2\pi}}{H} \frac{u_n(\xi_0)u_n(\xi)}{k_n^{1/2}} \right],$$

$$\text{dispersive spreading} = 10 \log \left(\frac{T_0}{T_0 + \Delta T_n} \right),$$

and

$$\text{cylindrical spreading} = -10 \log r.$$

Subtracting these terms from \bar{X}_i (expressed in dB relative to 1 dyne/cm²), gives the

$$\text{corrected signal} = S - \alpha_n r.$$

The three correction terms given above can be computed for each run from the range, the calculated mode shapes, and the group velocities.

It is assumed that α_n is fairly insensitive to the small changes in velocity profile and water depth observed in the course of the experiment, so that a plot of the corrected signal vs range should give a straight line with a slope equal to $-\alpha_n$. The corrected signal for the first mode is plotted vs range in Fig. 12. Some scatter is evident in the first-mode points at short ranges, but a reasonable straight line can be drawn which is also consistent with the source level S . The slope of this straight line gives 1.3 dB/km for the attenuation coefficient α_1 . This result is of the same order of magnitude as Tolstoy's results (3), obtained by other methods and under different conditions.

The second-mode corrected signals, plotted in Fig. 13, show an apparent increase with range, implying a negative attenuation coefficient. This result is believed due to the sensitivity of the "mode excitation function" correction with source position and the crudity of the dispersion correction. Unfortunately, for all of the runs except 2-1 the source was placed at a depth which was almost exactly on a zero of the second mode, leading to very large, negative corrections to the measured signal. In contrast, for the first mode the source position was very close to the maximum, where the mode amplitude changes slowly with depth. Thus the second-mode corrected signals are unreliable, although it is probably significant that run 2-1, for which the source was not so close to the zero, gives the lowest, and most reasonable, corrected signal.

It is clear that accurate measurements of all mode attenuation coefficients by this method should be made with both source and receiver near maxima of the desired mode. This means that knowledge of the approximate mode shape is necessary while the measurements are being made. In addition a better expression for the dispersion correction is needed, one which takes into account the actual pulse shape of the pressure signal at the source. We note in passing that we expect the attenuation coefficient of the second mode

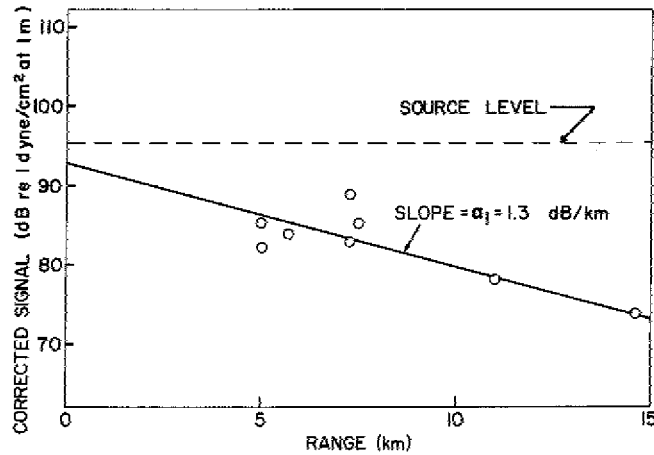


Fig. 12 - Measured signal level corrected for dispersion, cylindrical spreading, and calculated mode excitation for the first mode at 400 Hz. Numerical values are given in Table 2.

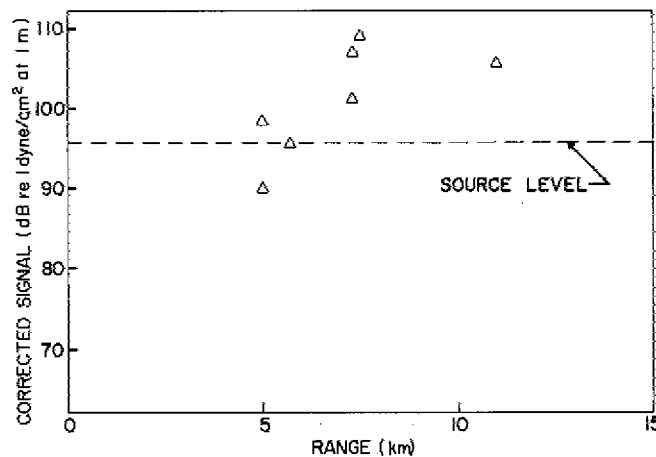


Fig. 13 - Measured signal level corrected for dispersion, cylindrical spreading, and calculated mode excitation for the second mode at 400 Hz. Numerical values are given in Table 2.

to be smaller than that of the first mode because of its smaller component in the bottom. Thus, it is reasonable that for run 2-1 the corrected signal for the second mode is higher than the first.

Oscillograph traces of the received signals for runs 12-3 and 12-4, 750 and 1500 Hz respectively, made under the same conditions as the previous 400-Hz example, are shown in Figs. 14 and 15, and the corresponding mode amplitudes and group velocities are shown in Figs. 16 and 10. Both measured patterns are quite complex; it was not possible to identify any modes for either frequency. Reference to the group-velocity curves indicates that most of the modes at 750 Hz, and the low-order modes at 1500 Hz, are overlapping, which implies that the observed patterns are partially due to interferences.

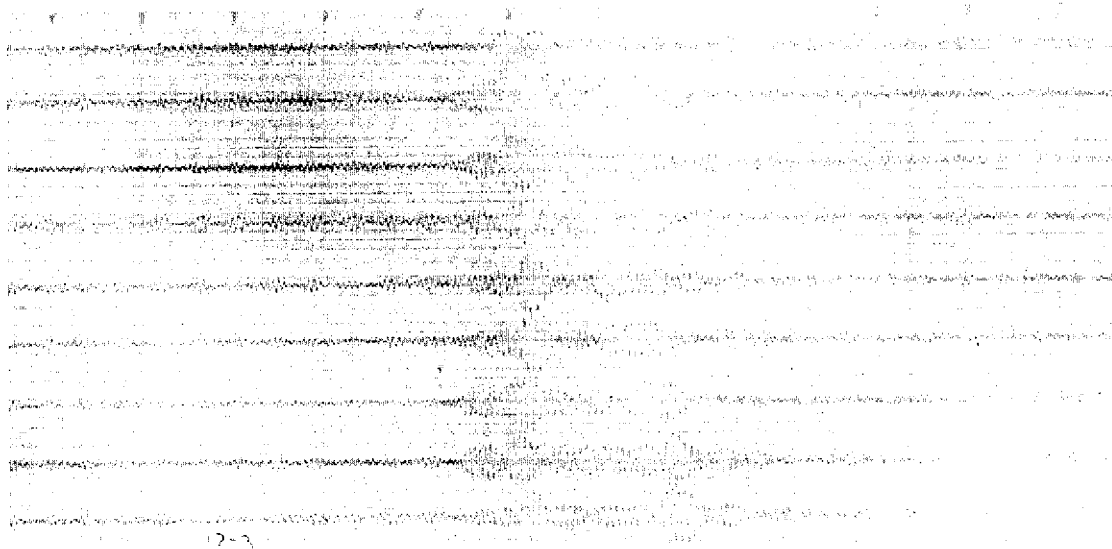


Fig. 14 - An example of a 750-Hz 3-cycle pulse received during run 12-3. The range was 11 km, and the source depth was 24.3 m. No individual modes could be identified.

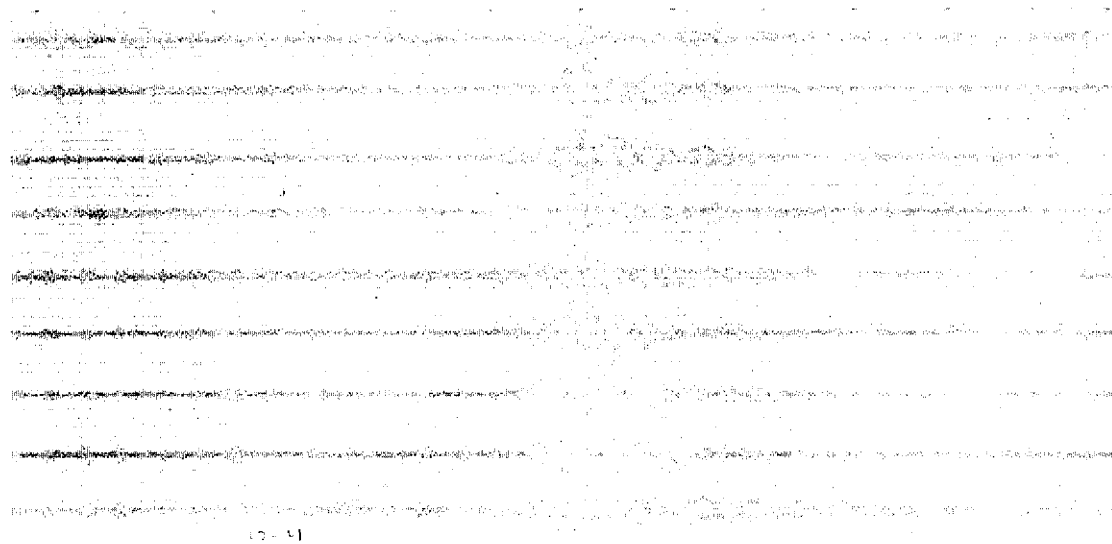


Fig. 15 - An example of a 1500-Hz 3-cycle pulse received during run 12-4. The range was 11 km, and the source depth was 22.9 m. No individual modes could be identified.

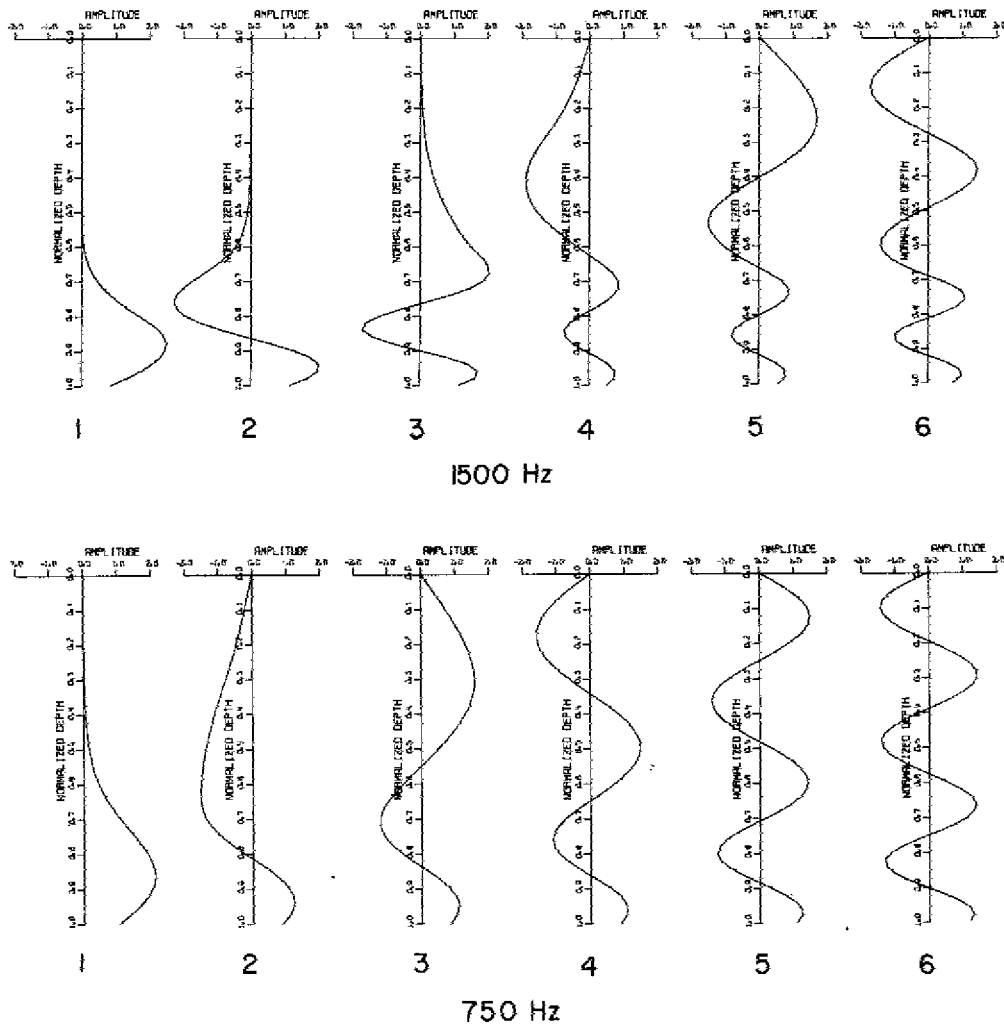


Fig. 16 - Mode amplitudes $u_n(t)$ for 750 Hz and 1500 Hz, calculated from the profile of BT 67 and Nansen cast 14 (profile shown in Fig. 8)

CONCLUSIONS

The results of this experiment indicate that, subject to the limitations imposed by environmental conditions, the short-pulse technique is a practical means of making direct measurements of the attenuation coefficients associated with individual modes of propagation. Although not every mode is resolvable under each set of environmental conditions, measurements made on those which are resolvable should serve to validate other less direct methods of measurement.

The simple normal-mode model used to predict modal group velocities and vertical pressure profiles proved to be adequate for this purpose for the first and second modes at 400 Hz. Results at 750 and 1500 Hz, where the low-order modes were consistently overlapping, are inconclusive.

The attenuation coefficient for the first mode at 400 Hz was calculated to be 1.3 dB per kilometer. Since the source was located near a null in the amplitude function for the second mode, the measurement of the coefficient was subject to large experimental error;

consequently a reliable value was not obtained for this mode. It was evident, however, that the second mode was attenuated less than the first. This is consonant with the predicted field distribution, if it is assumed that attenuation is primarily associated with the bottom.

ACKNOWLEDGMENTS

We thank A. O. Williams, Jr., for valuable discussions on the theoretical aspects of the problem, J. Cybulski and A. V. Newman for developing the normal-mode computer program, and the Naval Ship Research and Development Laboratory, Panama City, for support services furnished and for the use of their facility, Stage I.

REFERENCES

1. I. Tolstoy and C.S. Clay, "Ocean Acoustics," McGraw-Hill, 1966:
 - a. Chapter 4
 - b. p. 84
 - c. p. 133
2. R.H. Ferris and W. Kuperman, "An Experiment on Acoustic Reflection From the Sea Surface," NRL Report 7075, May 28, 1970
3. I. Tolstoy, J. Acoust. Soc. Amer. 30, 348 (1958)

Appendix A

THE NORMAL-MODE PROGRAM

The NRL normal-mode program solves Eqs. (4) numerically subject to the boundary conditions, Eqs. (5). The outputs consist of the functions $u_n(\zeta)$ in tabular or graphical form, the numbers k_n , and, optionally, the group velocities $U_n = \partial\omega/\partial k_n$. The program assumes that the sound velocity in the bottom c_2 is a constant and that the sound velocity in the water layer $c_1(\zeta)$ is given as a set of discrete values and associated water depths. The other required parameters are the frequency $\omega/2\pi$ and the water depth H .

For trapped modes $k_n > \omega/c_2$, and the solution of Eq. (4b) is

$$Z_n^{(2)}(\zeta) = B e^{-H[k_n^2 - (\omega^2/c_2^2)]^{1/2} \zeta}, \quad (\text{A1})$$

where B is an arbitrary constant. It follows from Eqs. (5b) and (5c) that

$$Z_n^{(1)}(1) = \frac{\rho_2}{\rho_1} B e^{-H[k_n^2 - (\omega^2/c_2^2)]^{1/2}} \quad (\text{A2})$$

and

$$\left. \frac{dZ_n^{(1)}}{d\zeta} \right|_{\zeta=1} = -BH[k_n^2 - (\omega^2/c_2^2)]^{1/2} e^{-H[k_n^2 - (\omega^2/c_2^2)]^{1/2}}. \quad (\text{A3})$$

For convenience we choose

$$B = -H^{-1} [k_n^2 - (\omega^2/c_2^2)]^{-1/2} e^{H[k_n^2 - (\omega^2/c_2^2)]^{1/2}}, \quad (\text{A4})$$

which gives

$$Z_n^{(1)}(1) = -\frac{\rho_2}{\rho_1} H^{-1} [k_n^2 - (\omega^2/c_2^2)]^{-1/2} \quad (\text{A5})$$

and

$$\left. \frac{dZ_n^{(1)}}{d\zeta} \right|_{\zeta=1} = 1. \quad (\text{A6})$$

The normalized water depth is divided into N specified intervals of equal length, and the differential Eq. (4a) is replaced by the approximate finite difference equation

$$[Z_n^{(1)}]_{i+1} = (2 - h^2 x_i^2) [Z_n^{(1)}]_i - [Z_n^{(1)}]_{i-1}. \quad (\text{A7})$$

In Eq. (A7) the subscript i indicates that the function is to be evaluated at the endpoint of the i th interval, with the length of an interval being $h = 1/N$. The function x_i^2 is defined as

$$x_i^2 = H^2 \left[\left(\frac{\omega^2}{[c_1^2]_i} \right) - k_n^2 \right], \quad (\text{A8})$$

where $[c_1^2]_i$ is obtained by linear interpolation of the input values of c_1 .

Two points are necessary to begin the calculation; $[Z_n^{(1)}]_0$ is given by Eq. (A5), and $[Z_n^{(1)}]_1$ is obtained from a Taylor series expansion of $Z_n^{(1)}(\zeta)$ about the point $\zeta = 1$. Making use of Eqs. (A5) and (A6) we get, to terms of order h^2 ,

$$[Z_n^{(1)}]_1 = h + \left(\frac{h^2 x_0^2}{2} - 1 \right) \frac{\rho_2}{\rho_1} H^{-1} [k_n^2 - (\omega^2/c_2^2)]^{-1/2}. \quad (\text{A9})$$

The procedure then is as follows: A trial value of k_n^2 is chosen, and $Z_n^{(1)}(1) = [Z_n^{(1)}]_0$ and x_0^2 are computed; then $[Z_n^{(1)}]_1$ is computed from Eq. (A9). Next x_1^2 is computed and inserted into Eq. (A7) along with $[Z_n^{(1)}]_0$ and $[Z_n^{(1)}]_1$, which then gives $[Z_n^{(1)}]_2$. Then x_2^2 is computed and inserted into Eq. (A7) along with $[Z_n^{(1)}]_1$ and $[Z_n^{(1)}]_2$ to obtain $[Z_n^{(1)}]_3$. The procedure is repeated until $[Z_n^{(1)}]_N$ is reached. A check is made to determine if $[Z_n^{(1)}]_N$ satisfies the condition

$$[Z_n^{(1)}]_N < \kappa [Z_n^{(1)}]_0, \quad (\text{A10})$$

where κ is a small number chosen so that the boundary condition Eq. (5a) is approximately satisfied. If Eq. (A10) is not satisfied, a new trial value of k_n^2 is chosen and the entire calculation is repeated. When Eq. (A10) is satisfied, the value of k_n^2 and the set of numbers $[Z_n^{(1)}]_i$, $0 \leq i \leq N$, are taken to be the required solution.

The eigenfunctions are then normalized by using Eq. (3), calculating the first integral numerically and using the exact value of $Z_n^{(2)}(\zeta)$ given by Eq. (A1) in the second integral. Examples of the resulting normalized eigenfunctions $u_n(\zeta)$, which we have called mode amplitudes, are given in Fig. 9.

The group velocities, defined by

$$U_n = \frac{\partial \omega}{\partial k_n}, \quad (\text{A11})$$

are calculated by numerical differentiation of k_n with respect to ω , k_n being computed for a suitable number of frequencies over the desired range. Examples of the calculated group velocities are given in Fig. 10.

Appendix B

OCEANOGRAPHIC MEASUREMENTS

INTRODUCTION

In addition to the acoustic measurements a sizable number of oceanographic data were collected during this experiment. Table B1 gives time and position of the bathythermographs (BT's), Nansen casts, and velocimeter casts taken aboard the ship and the BT's taken from Stage I (denoted in the table by numbers prefixed with a "P").

The geographic positions of the oceanographic measurements are shown in Fig. B1. These data were taken primarily to obtain sound-speed profiles to be used by the normal-mode computer program in predicting mode amplitudes and group velocities. Once calibrated, the velocimeter proved to be a simple and repeatable instrument for obtaining these profiles; however, mechanical problems prevented its use while the hydrophone string was in the water. Since Nansen casts and BT's could be taken with the hydrophones in the water, sound-speed profiles derived from them using Wilson's equation* were used for the normal-mode program when BT's taken during a lengthy acoustic run indicated that the profile had changed significantly since the last velocimeter cast.

Although not all of the data taken were actually used to compute sound-speed profiles for the program, we will present here the entire body of oceanographic data collected in the expectation that the information it contains on temporal stability of the ocean's temperature and salinity structures may be of interest to future investigators working in this area.

TEMPERATURE MEASUREMENTS

Photographs of the 67 bathythermograms taken from the ship and the ten taken from the platform, superimposed on the appropriate depth-temperature grid, are presented in Fig. B2. The two 200-foot bathythermographs used aboard ship were checked for temperature accuracy by comparing their readings with those taken from reversing thermometers attached to Nansen bottles (from two to six of the bottles on any given Nansen cast carried these thermometers). Temperatures taken by the BT's and reversing thermometers agreed quite well in the isothermal layers typically found near the surface and near the bottom, with the BT's averaging slightly less than 0.1° F higher.

SALINITY MEASUREMENTS

Salinity profiles derived from water samples taken by the 14 Nansen casts are shown in Fig. B3. A total of 163 water samples, from two to 18 per cast, were processed on a portable induction salinometer (Industrial Instruments, Inc., Model RS-7B). The range of salinities encountered was quite large, from 32.51 to 36.15 parts per thousand. The salinity profiles generally have two isosalinity layers separated by a strong positive gradient.

*W.D. Wilson, J. Acoust. Soc. Amer., 23, 1357 (1960).

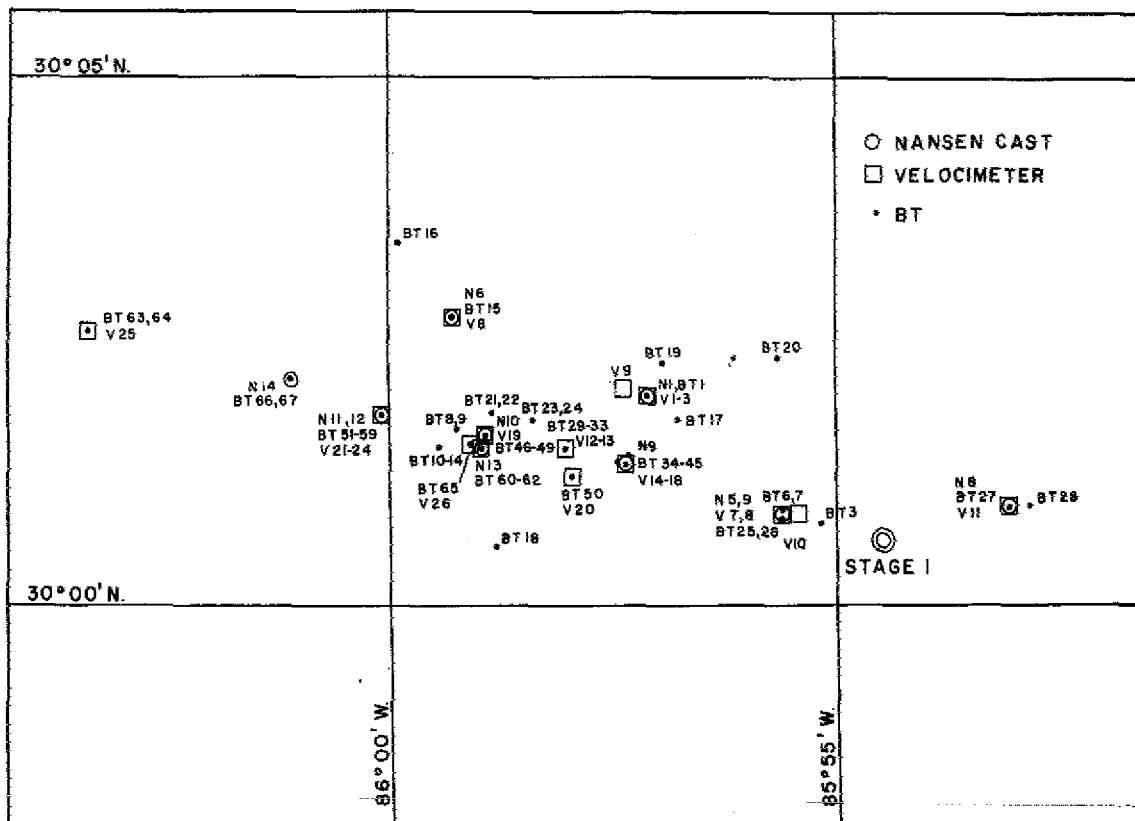


Fig. B1 - Geographic location of BT's, Nansen casts, and velocimeter casts taken during this experiment. BT's 2, 4, and 5, Nansen casts 2, 3, and 4, and velocimeter casts 4, 5, and 6 were taken at ranges of 28.1 to 31.2 km, and bearings of 283.5 to 295 degrees from Stage I and do not appear on this chart; they would appear at about twice the position of BT's 63 and 64 and velocimeter cast 25 relative to Stage I.

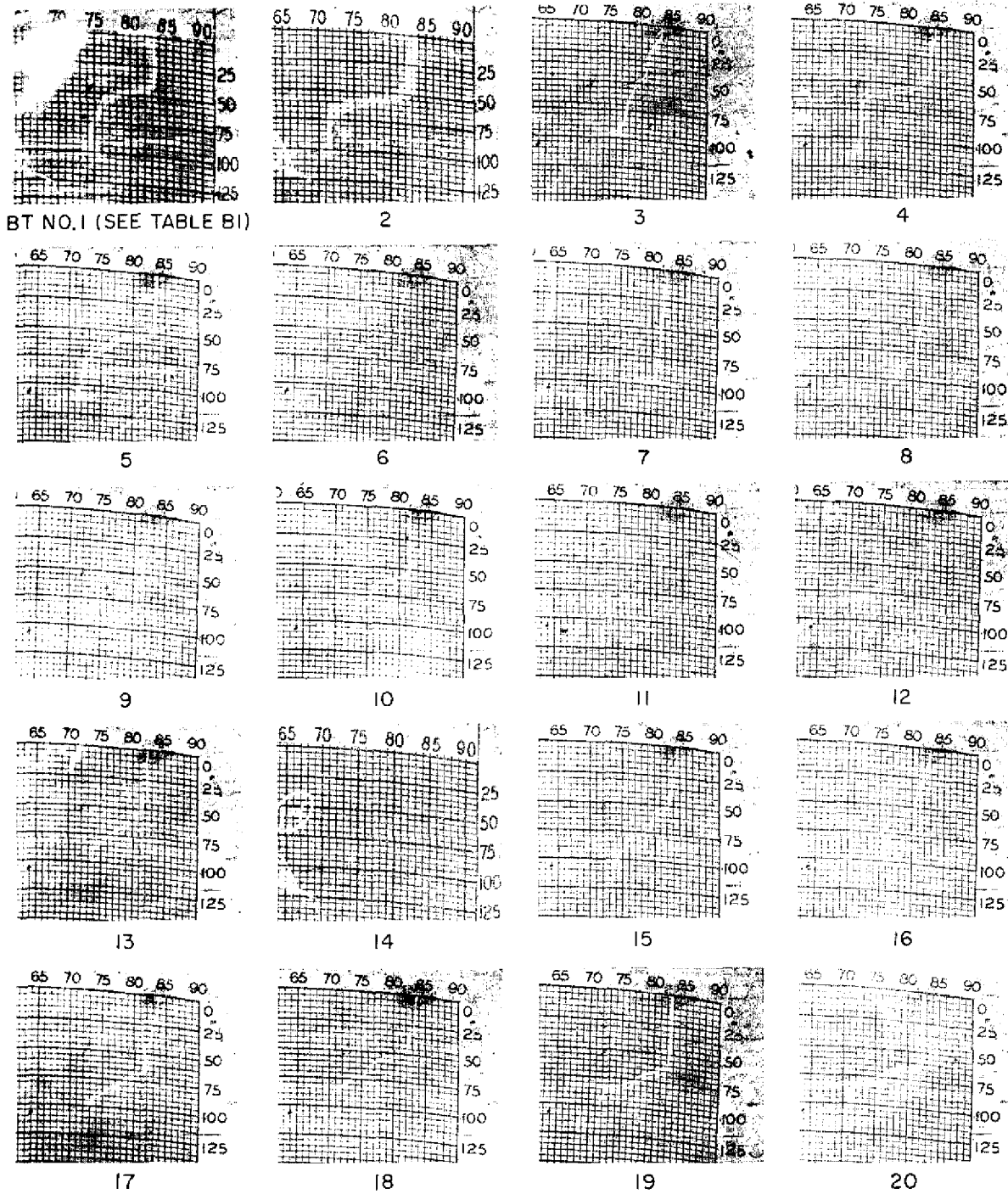


Fig. B2 - Bathythermograms taken during the experiment (depth in feet and temperature in degrees Fahrenheit)

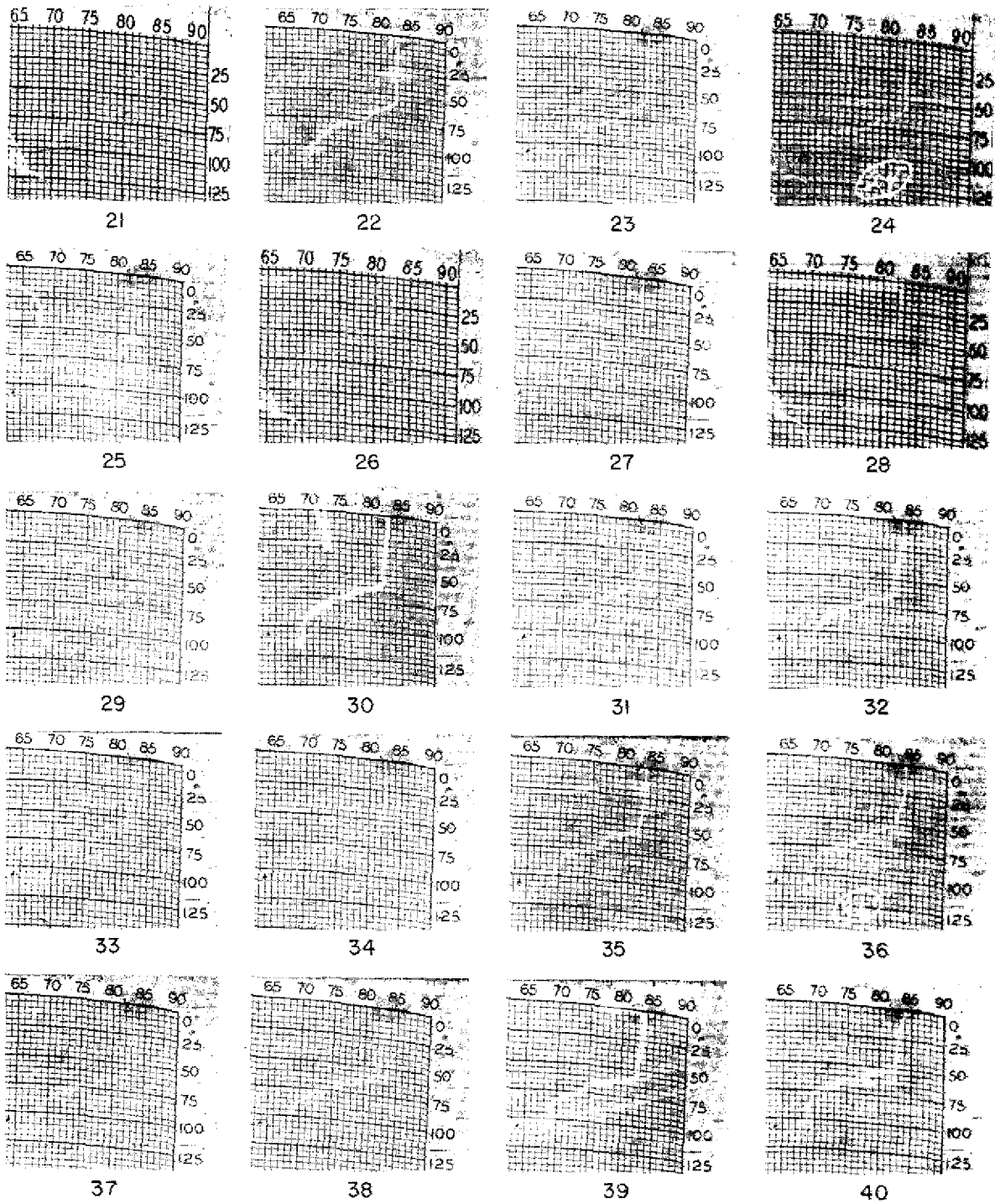


Fig. B2 (Continued) - Bathythermograms taken during the experiment (depth in feet and temperature in degrees Fahrenheit)

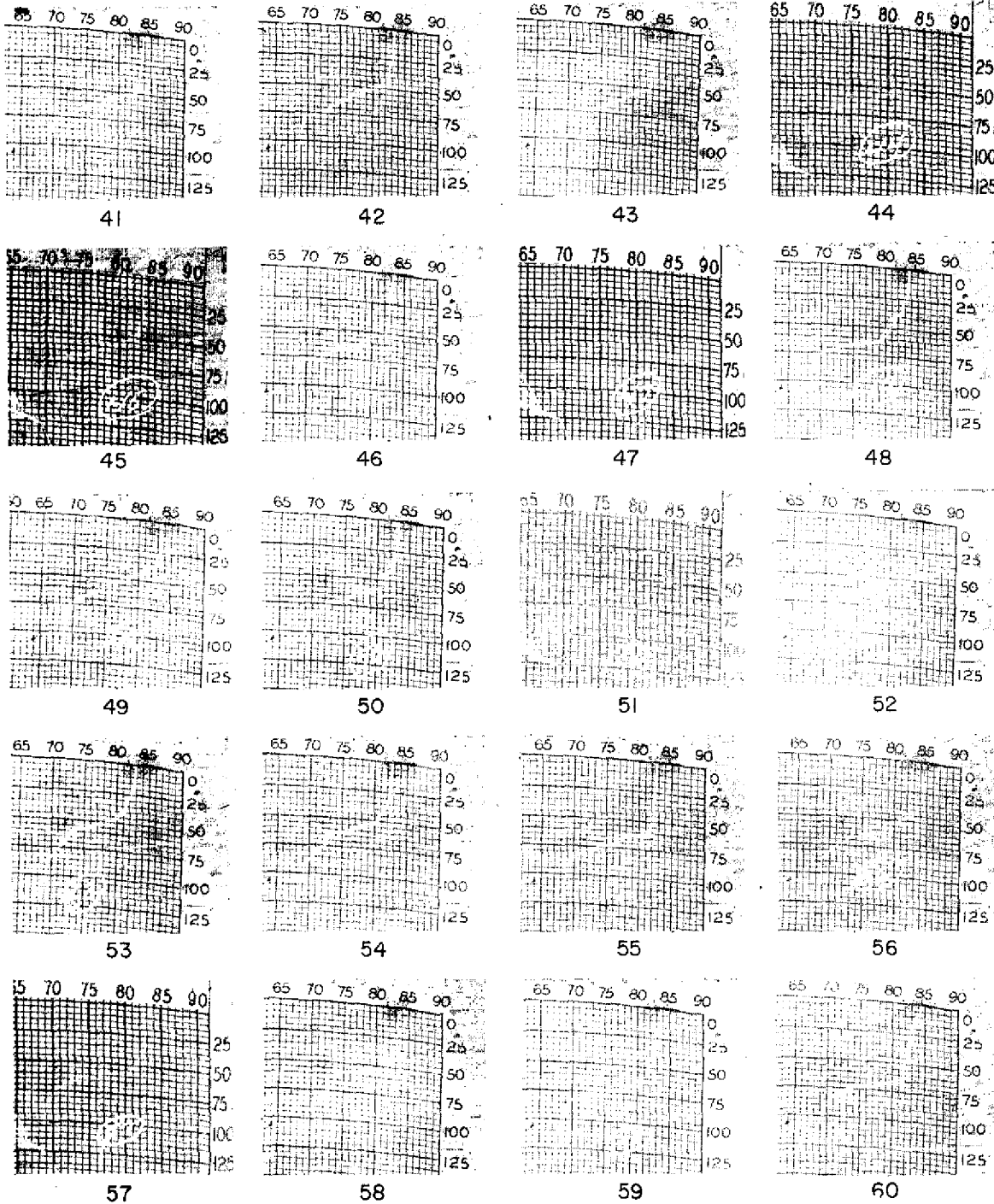


Fig. B2 (Continued) - Bathythermograms taken during the experiment (depth in feet and temperature in degrees Fahrenheit)

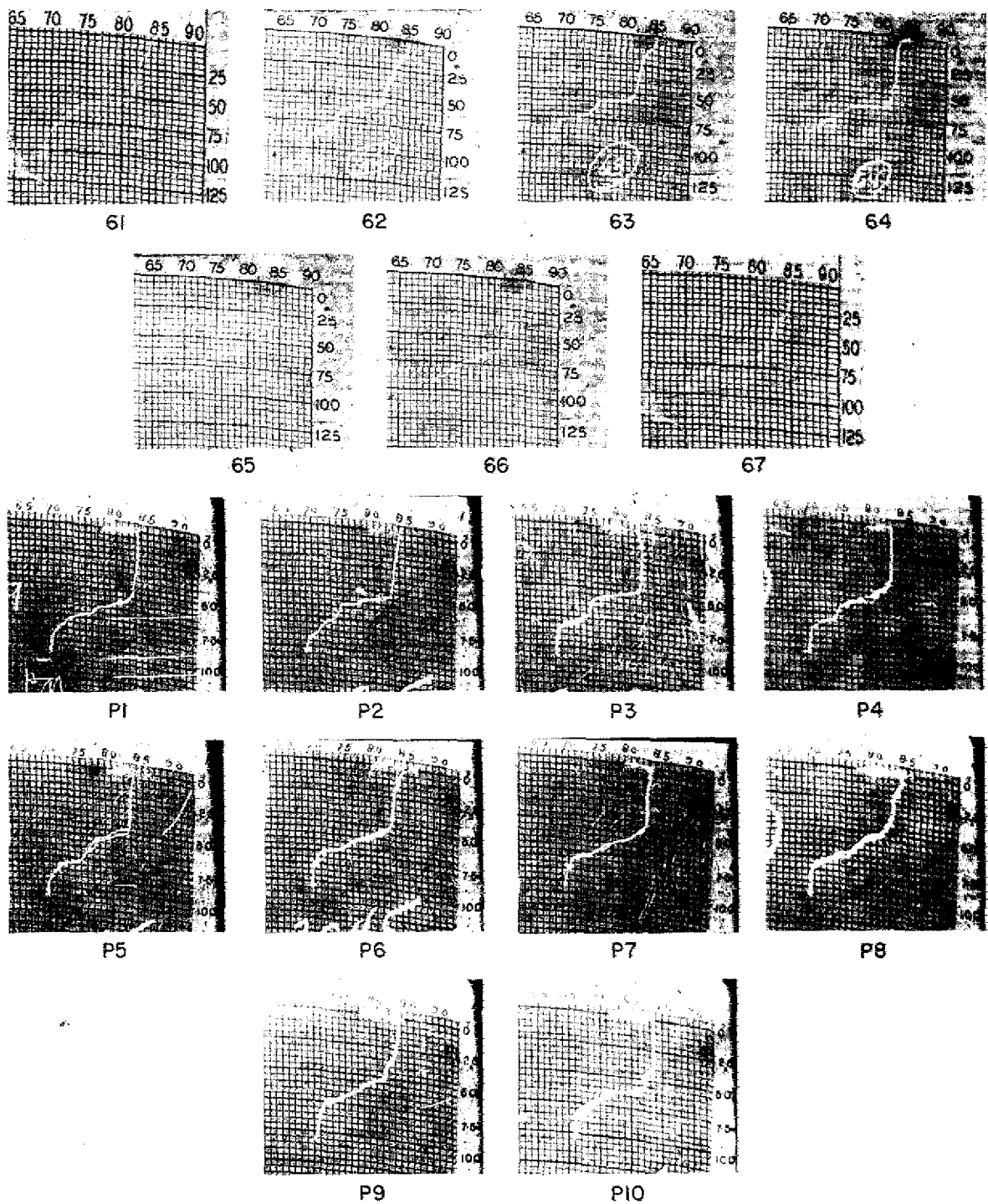


Fig. B2 (Continued) - Bathythermograms taken during the experiment (depth in feet and temperature in degrees Fahrenheit)

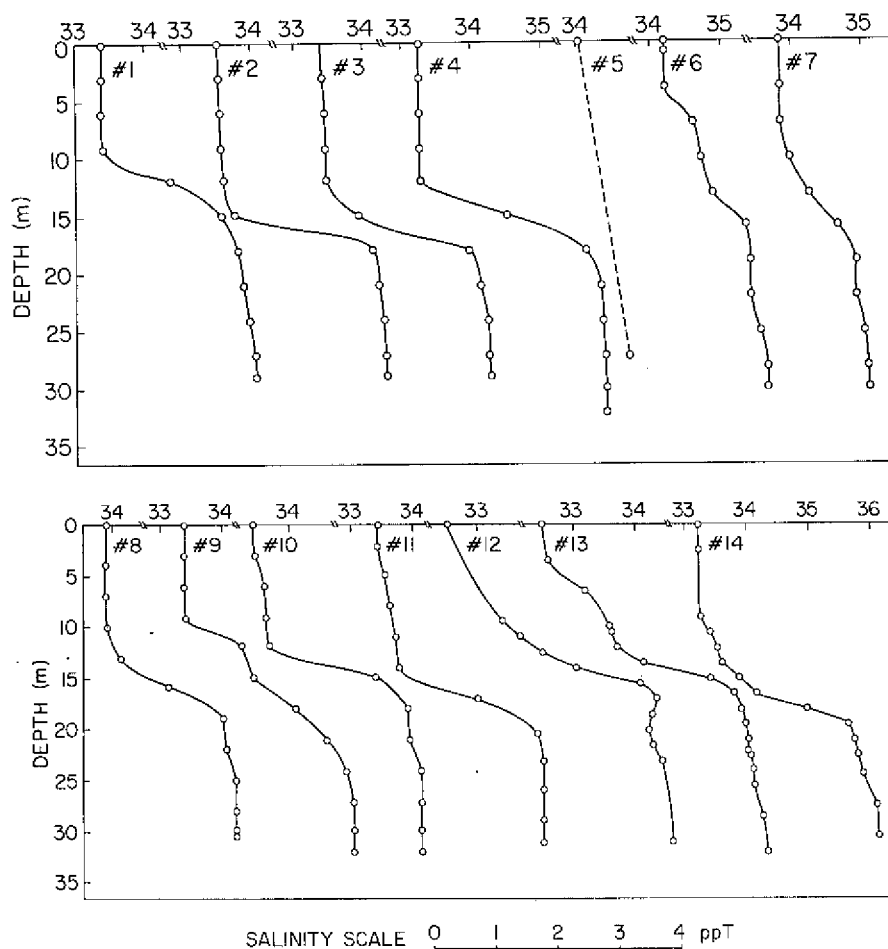


Fig. B3 - Salinity profiles computed from the water samples brought up by the Nansen bottles. The identification numbers refer to Table B1. The salinity values are in parts per thousand.

SOUND-SPEED MEASUREMENTS

A "sing-around" velocimeter, model TR4-D (M4) made by ACF Industries, was used to obtain sound-speed profiles directly. Since current calibration constants were not available for this unit, it was calibrated at sea by comparing the output frequency of the velocimeter with sound speed computed from Nansen-cast salinity values and BT surface thermometer readings. Frequencies read while the velocimeter was held just below the surface at the beginning and end of velocimeter casts 4, 6, 7, 8, 10, and 11 were compared with sound speeds computed from temperature and salinity data taken during the velocimeter run (except in the case of velocimeter cast 7, for which the relevant Nansen cast was taken 40 minutes later). This generated 11 ratios of sound speed to velocimeter frequency output (one bad reading being rejected). The mean of the 11 ratios was 206.62 m/sec per kHz, and their standard deviation was 0.03 m/sec per kHz. Accordingly, the equation used to convert velocimeter readings was

$$\text{sound speed (m/sec)} = 206.62 \times \text{velocimeter frequency output (kHz)}.$$

A more rigorous calibration would include at least two calibration constants, but the simplified equation used here is adequate for the limited range of sound speeds encountered.

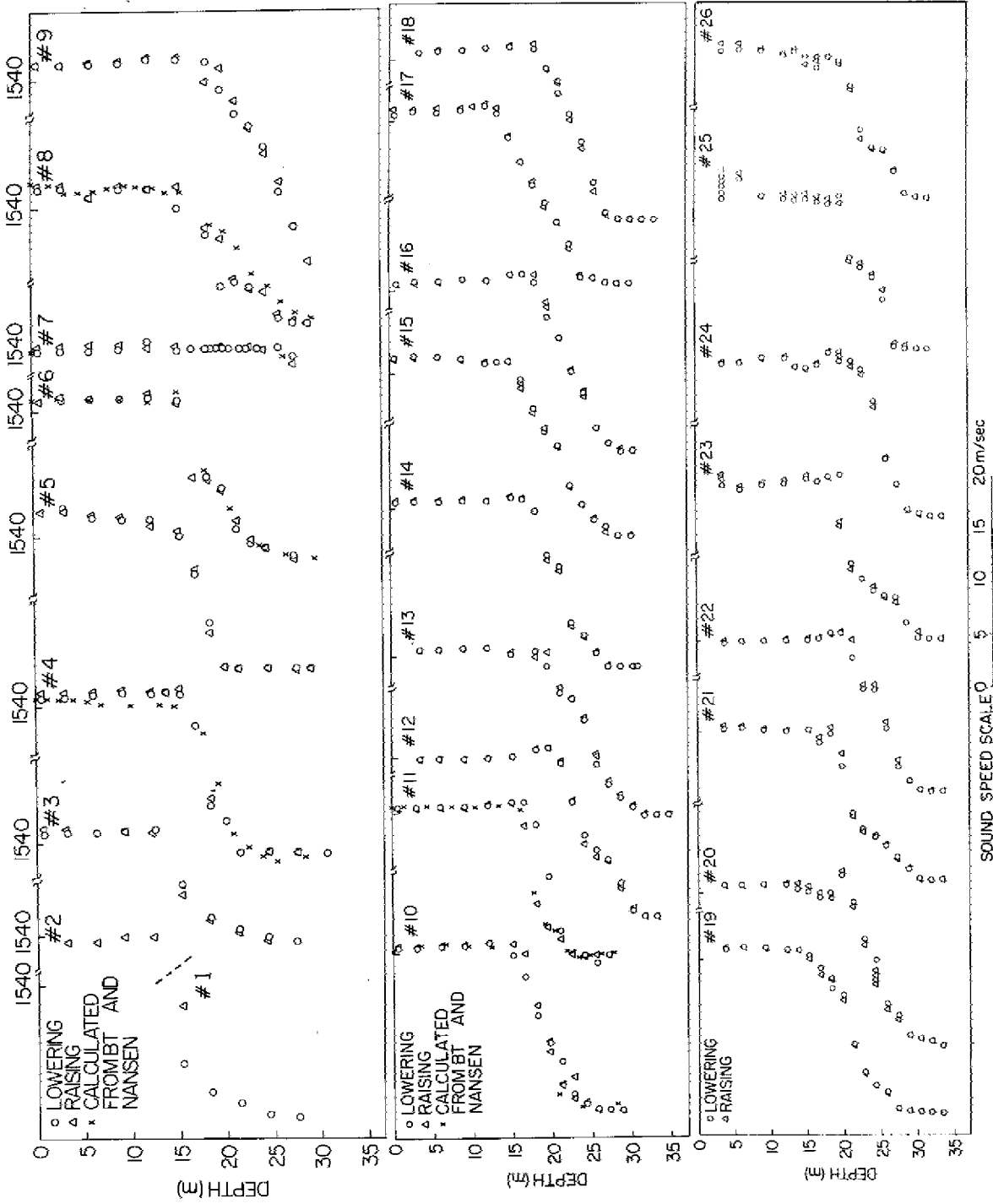
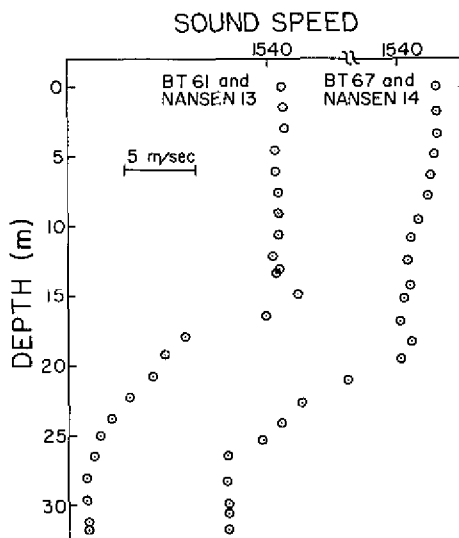


Fig. B4 - Velocimeter data taken during the experiment. The identification numbers refer to Table B1.

Fig. B5 - Sound speed profiles obtained from BT's and Nansen casts taken during runs 9-6 (left) and 12-2 (right) listed in Table 2. Velocimeter casts were not made during these runs.



For each velocimeter cast the instrument was lowered to the bottom in 5-foot depth increments; it was allowed to stabilize at each depth, and the output frequency was counted for 10 seconds. The measurement was repeated at each depth on the way up, and both sets of data are plotted for each cast in Fig. B4. In addition, for the six cases where a BT and Nansen cast were obtained simultaneously, calculated Wilson's equation profiles are presented.

For two of the acoustic runs for which mode-attenuation data will be found in Table 2 the relevant sound-speed profiles were obtained from BT's and Nansen casts. These profiles are shown in Fig. B5.

WAVE-STAFF MEASUREMENTS

The voltage output from a resistance-type wave staff attached to one of the legs of Stage I was recorded on magnetic tape during most data runs. The root-mean-square wave amplitudes about the mean water level for surface waves with frequencies below 0.5 Hz are presented in Table B2 for wave-staff recordings made within approximately 1 hour of acoustic runs 9-6, 11-3, 11-5, and 12-2, 3, 4.

Table B2
Wave-Staff Measurements of the
Sea Surface at Stage I Within
1 Hour of the Acoustic Run

Date	Time (CDT)	Acoustic Runs	RMS Amplitude of Waves With $f < 0.5$ Hz (cm about mean water level)
8/1/69	1150	9-6	8
8/1/69	1900	11-3	7
8/2/69	1217	11-5	16
8/2/69	1710	12-2, 3, 4	15